



Gauchotte-Lindsay, C., and Turnbull, S. M. (2016) On-line high-precision carbon position-specific stable isotope analysis: a review. *Trends in Analytical Chemistry*, 76, pp. 115-125.

There may be differences between this version and the published version. You are advised to consult the publisher's version if you wish to cite from it.

<http://eprints.gla.ac.uk/117118/>

Deposited on: 5 May 2016

Enlighten – Research publications by members of the University of Glasgow
<http://eprints.gla.ac.uk>

1 **On-line high-precision carbon position-specific stable isotope analysis - A review.**

2 Caroline Gauchotte-Lindsay*, Stephanie M Turnbull

3 Infrastructure and Environment Research Division, School of Engineering,
4 University of Glasgow, Rankine Building, Oakfield Avenue, Glasgow, UK, G12
5 8LT.

6 * Corresponding author: Email: caroline.gauchotte-lindsay@glasgow.ac.uk, Tel:
7 0141 330 3842

8 **Abstract**

9 Since the first commercial availability of gas chromatographs coupled with a
10 combustion furnace and an isotope ratio mass spectrometer in 1990, compound
11 specific stable isotope analysis of organic molecules has been at the origin of
12 scientific breakthroughs in a wide range of research fields. The presence of non-
13 reacting atoms, however, can mask changes in molecular stable isotopic signatures;
14 position specific isotope analysis (PSIA) is the study of *intramolecular* isotopic
15 variations. After considering briefly the potential and prospect of this new level in
16 isotopic studies, we review here the handful of existing custom-built systems for on-
17 line PSIA using continuous flow isotope ratio mass spectrometry instrumentation and
18 how researchers have addressed issues specific to the technique. We also discuss the
19 various molecular fragmentation processes observed and optimised for various
20 molecules for on-line PSIA as it should help to inform application to new compounds.

21 **Abbreviations**

22 GC, Gas chromatography; GC-c-IRMS, Gas chromatography coupled with
23 combustion furnace and isotope ratio mass spectrometry; BSIA, Bulk stable isotope
24 analysis; CSIA, Compound specific isotope analysis; PSIA, Position specific isotope
25 analysis; IRMS, Isotope ratio mass spectrometry; CF, Continuous flow; NMR,
26 Nuclear magnetic resonance; SNIF-NMR, Site specific natural isotope fractionation
27 nuclear magnetic resonance; EA-IRMS, Elemental Analysis - Isotope Ratio Mass
28 Spectrometry; GC-Py-IRMS, Gas chromatography-pyrolysis-isotope ratio mass
29 spectrometry; FID, Flame ionisation detector; FAMEs, fatty acid methyl esters;
30 MTBE, methyl *tert* butyl ether; f, remaining fraction of reactant; KIEs, Kinetic
31 isotope effects; AKIE, Apparent kinetic isotope effect; UVA, ultra violet

32
33
34

35 **Keywords**

36 Gas chromatography coupled with isotope ratio mass spectrometry; Bulk stable
37 isotope analysis; Compound specific isotope analysis; Position specific isotope
38 analysis; Isotope ratio mass spectrometry; Fluxomics
39

40 **1 Introduction**

41 There are three levels of specificity for stable isotope analysis: bulk stable isotope
42 analysis (BSIA) [1], compound specific isotope analysis (CSIA) [2] and position
43 specific isotope analysis (PSIA) [3] (Table 1). Historically, for isotope ratio analysis,
44 the samples were quantitatively converted off-line to simple gases (CO₂ or CO and N₂
45 for carbon and nitrogen analysis and H₂ and CO for oxygen and hydrogen analysis)
46 and then introduced to an isotope ratio mass spectrometer (IRMS) via an introduction
47 system called dual-inlet. In the IRMS, the isotopic signatures were compared to
48 calibrated gas standards. Dual-inlet analysis allows very precise and accurate stable
49 isotope ratio analysis but requires large volumes of sample and tedious pre-analysis
50 sample treatments [3]. The development of the continuous flow introduction system
51 (CF) has enabled the direct analysis of much smaller sample volumes [3, 4]. The
52 carrier gas (helium) carries the analyte in the gaseous phase into the ion source of the
53 mass spectrometer. It has allowed the connection of IRMS to different automated
54 sample preparation devices.

55 The magnitude of isotopic fractionation is greatest at the site of reaction in the
56 molecule [5] and it has been accepted for a long time that *intramolecular* isotopic
57 distribution was not homogeneous [6]. Position specific isotope analysis (PSIA) is the
58 term that refers to the study of *intramolecular* isotopic variations within a molecule.
59 Abelson and Hoering [7] presented the very first study on *intramolecular* isotopic
60 variations. Using the nihydrin reaction, they performed the decarboxylation of several
61 amino acids, collected the liberated CO₂ and measured its carbon stable isotope ratios
62 by dual-inlet IRMS. The carboxyl groups showed great variability in function of the
63 origin of the amino acids and in most cases were greatly enriched compared to the rest
64 of the molecule. For the first time, the non-homogeneous isotopic distribution inside a
65 molecule was revealed and the relationship between the origin of the molecule and the
66 *intramolecular* isotopic variations was demonstrated. Abelson and Hoering also
67 established that for PSIA, the reaction breaking down the molecule had to be

68 quantitative (total) so the isotope ratios of the fragments are representative of the
69 moieties in the parent molecule. Although the off-line isolation of functional groups
70 of interest by chemical reaction (chemolysis) provides precise intramolecular isotope
71 analysis, it has not been widely used since Abelson and Hoering [7]. The few existing
72 PSIA studies, however, consistently demonstrated that the carbon isotopic distribution
73 in a molecule was heterogeneous and depended on its origin [6, 8]. Nuclear magnetic
74 resonance (NMR) has also been used to determine site specific isotope signatures. The
75 technique called site specific natural isotope fractionation nuclear magnetic resonance
76 (SNIF-NMR) enabled to directly access site specific isotope ratio by identification
77 and quantification of isotopomers by NMR [9]. It is widely used to determine D/H
78 [10] ratios but has also been used for the determination of $^{13}\text{C}/^{12}\text{C}$ ratios [11]. Both
79 off-line chemical reactions and NMR for position specific isotope analysis require a
80 pure sample and therefore necessitate complicated extraction prior to analysis in very
81 large sample sizes for accurate measurements [5]. NMR is however capable of
82 producing results which are now comparable in accuracy to *intramolecular* isotope
83 composition results obtained via IRMS analysis [5, 12].

84 Various reviews have extensively presented the wide range of the applications of
85 CSIA ranging from archaeology to sport and including geo and extra-terrestrial
86 chemistry, forensic and biomedical sciences [4, 13]. And in the same manner as CSIA
87 greatly enhanced the resolution power of stable isotope analysis compared to BSIA,
88 PSIA is the next resolution level. Brenna *et al.* [14] demonstrated in a review how
89 natural *intramolecular* isotope measurements could help advance the field of
90 physiology alongside other emerging techniques such as genomics and proteomics.
91 Elsner *et al.* [15] identified PSIA as the next level of analysis for mechanistic isotopic
92 fractionation studies of organic contaminants while Burton *et al.* [16] propose the use
93 of the technique to identify the origin of the various carbon atoms in extra-terrestrial
94 amino acids.

95 CF technologies enabled the development of on-line CSIA systems, which in turn
96 triggered a rapid expansion of the method and its applications. On-line preparation of
97 samples for PSIA using CF-IRMS is therefore theoretically possible too. However,
98 while hyphenated IRMS instrumentations for on-line CSIA [2] have been available
99 commercially since 1990 and are now widely employed, only a handful of
100 laboratories carry out on-line PSIA for stable carbon isotope analysis on custom-built
101 CF-IRMS instrumentations. In this review our aim is to introduce online-PSIA and

102 encourage further developments of this high-potential technique. To this aim, after
103 discussing some current examples of PSIA applications and the potential of the
104 technique as complementary to CSIA, we will present the existing CF-IRMS systems
105 and their specific characteristics, advantages and drawbacks and inventory and
106 categorize the reported mechanisms of on-line gaseous thermolysis of various
107 compounds for on-line PSIA. This will also include discussions on how, for different
108 systems and different fragmentation mechanisms, general issues such precision and
109 sensitivity and issues more specific to PSIA such as isotopic fractionation and
110 representativeness have been addressed.

111

112 **2 Basics in position specific stable isotope analysis**

113 We present here an overview of the fundamentals in stable isotope analysis at natural
114 abundance level necessary to the understanding of this review, more detailed
115 information can be found elsewhere (see for instance[1]).

116 The abundance of a stable isotope of an element, or the probability that an atom is of a
117 particular isotope among the population of a given element, is represented either by
118 the ratio (R) or the fraction (F) between the concentrations of the heavy (H) and the
119 light (L) isotopes (Equation (1)).

$$R = \frac{H}{L} \text{ and } F = \frac{H}{L+H} \quad (1)$$

122 Isotope ratios, however, are conventionally expressed in delta (δ) notations relative to
123 an international standard to facilitate inter-laboratory comparisons. They are relative
124 values where the isotopic composition of a sample is compared to the isotopic
125 composition of the standard and they are expressed in per mil (‰) (Equation (2)).

$$126 \quad \delta H = \left(\frac{R_{\text{sample}} - R_{\text{standard}}}{R_{\text{standard}}} \right) \times 1000 \quad (2)$$

127 Chemical reactions, natural or anthropogenic, change the isotopic distribution of a
128 molecule. It is predicted by statistical models that lighter isotopes form weaker bonds
129 and therefore are more reactive than the heavier isotopes [5]. Consequently, the rate of
130 a chemical reaction will be slower for molecules in which one of the atoms of the
131 reactive bond is a heavy isotope; in general, this implies that the products of a reaction
132 will contain a higher concentration of the lighter isotope, while reactants will be
133 concentrated in the heavier isotope [5]. The change in relative abundances of stable

134 isotopes of an element due to a mass discriminatory process is termed isotopic
 135 fractionation. In a closed reversible system where the source of reacting substrate is
 136 not renewed the fractionation factor, α , is defined as the ratio of the R values of the
 137 products formed in an infinitely short time over that of the reactant. The kinetic
 138 isotope effects (KIEs) describe the ratios in reaction rate constant between molecules
 139 with ^{12}C and ^{13}C at the reactive position.

140

141 The fractionation factor, the remaining fraction of reactant (f) and the change in
 142 isotopic signature of the reactant during the reaction are all linked by the Rayleigh
 143 equation, an adaptation of Lord Rayleigh's equation on the fractionation of two
 144 compounds during distillation (Equation (3))[17]):

$$145 \quad \ln\left(\frac{\delta H + 1000}{\delta H_0 + 1000}\right) = (\alpha - 1) \ln f = \frac{\varepsilon}{1000} \ln f \quad (3)$$

146 With δH_0 the isotopic signature of the reactant before the start of the reaction and ε ,
 147 equal to $1000(\alpha - 1)$ the enrichment factor.

148 .

149 The enrichment factor of a reaction can be determined experimentally through linear
 150 regression of $\ln(\delta H + 1000 / \delta H_0 + 1000)$ versus $\ln(f)$ in a controlled reaction.. It can then
 151 be used to calculate a value coined by authors [18] the apparent kinetic isotope effect
 152 (AKIE) using the following equation (Equation (4)):

$$153 \quad \text{AKIE} = \frac{154}{1 + z \frac{x}{1000}} \quad (4)$$

157

158 n is the number of carbon atoms in the reacting molecule, with x of them are located
 159 at the site of reaction amongst which z are isotopically equivalent position. For
 160 primary isotope effect $z = x$. The term $(n/x)\varepsilon$ is called the intrinsic or position
 161 enrichment factor and is meant to correct for the dilution in the observed enrichment
 162 factor due to non-reacting positions; it is based on the assumption that isotopes are
 163 distributed evenly within molecules of a same compound. For detail calculations
 164 leading to Equation 4 please refer to the review by Elsner *et al* [15]. When several
 165 mechanisms are suspected for a given reaction, the AKIE can be calculated for each

166 possible pathway and compared to KIEs computationally calculated using the
167 Streitwieser Semiclassical Limits model [5] for various bond breaking/forming
168 reactions. Divergences between observed AKIEs and KIEs could therefore be
169 attributed to the assumption that stable isotopic signatures are homogeneous within a
170 molecule. PSIA has therefore the potential to give access experimentally to more
171 accurate AKIEs.

172
173

174 **3 Applications of PSIA**

175

176 PSIA allows observing and quantifying non-random distributions within molecules at
177 natural abundance levels. These distributions are a representation of the “history” of
178 natural and synthetic compounds: their synthesis and further transformations. At
179 compound level, internal variations might be diluted by unchanging ratios. PSIA, off-
180 line, on-line and using NMR, can be employed in two principal ways; 1) to
181 mechanistically study (bio)chemical reactions and elucidate pathways and 2) to infer
182 origins of chemically identical molecules of various origins including possible
183 adulteration. In the following section, without attempting to be exhaustive, we aim to
184 present examples of published applications of PSIA and particularly of on-line PSIA
185 in CF systems to demonstrate the usefulness and potential of the method.

186 **3.1 Origin and source inference**

187

188 Off-line PSIA methods and SNIF-NMR have been employed to investigate the origin
189 of natural and synthetic compounds. Particularly, ^2H -SNIF-NMR has been a very
190 successful method for the authentication of beverages and food [19]. It was even
191 adopted by the European Union in 1990 as the official method for the control of the
192 addition of sugars to wines pre-fermentation (or chaptalisation) ([19] and references
193 therein); the difference in position specific D/H ratio in the methyl and methylene
194 groups of the ethanol molecule permitting to differentiate between sugar-added and
195 natural wines. It has also been employed for the provenancing of illicit drugs [20]. For
196 instance, the molecule of heroin derived from the acetylation of morphine and out of
197 the 23 hydrogen atoms in a molecule of heroin, 15 are of natural origin and 8 of

198 “synthetic” origin; accessing their isotopic signature separately permit at the same
199 time to gather information on geographical origin of the drug and the commercial
200 source of its synthetic additive [20]. Recently, SNIF-NMR was extended to atoms
201 other than hydrogen. Bussy *et al.* [21] demonstrated notably the potential of carbon
202 position specific stable isotope analysis for the fingerprinting of active pharmaceutical
203 ingredients as a “tag” to combat counterfeiting as it could capture differences between
204 batches, manufacturing processes or origin in raw products.

205 As discussed previously, on-line CF methods are more compatible with complex low
206 concentration samples but their use has so far been limited for PSIA. With an on-line
207 PSIA system described in Section 4 (System 3 in Section 4) Hattori *et al.* [22] used
208 on-line pyrolysis of acetic acid to compare the $\delta^{13}\text{C}$ of the carboxyl and the methyl
209 carbon atoms of acetic acid in fourteen vinegars of various origins [22]. Thirteen out
210 of the 14 samples, exhibited acetic acid with a methyl carbon depleted compared to
211 the carboxyl carbon reflecting their biological origin. The last sample, however,
212 showed homogeneous carbon signature for the two positions unveiling a possible
213 addition of synthetic acetic acid to the vinegar. Gilbert *et al.* [23], using the same
214 system, analysed the intramolecular carbon stable isotope values of ethanol in various
215 alcoholic beverages and demonstrated that while the addition of C₄-based ethanol to
216 C₃-derived liquors could be detected at molecular level, *intramolecular* values for the
217 methanol and methyl groups in the ethanol molecule were necessary to detect addition
218 to CAM-derived beverages.

219 Using amino acids from various commercial sources, Brenna *et al.* compared
220 intramolecular isotopic variations with whole molecule variations [3]. Position
221 specific isotope analysis using System 4 (see Section 4) enabled to demonstrate that
222 the molecular variations were due to high variations at a restricted number of
223 positions [24]. PSIA also demonstrated that some of the amino acids from different
224 commercial distributors had the same sources or that a particular acid was not of
225 biological origin [24, 25].

226 Finally, on-line palladium catalysed decarboxylation of the low molecular weight
227 acids produced by hydrous pyrolysis of an oil-prone shale [26], in an early version of
228 System 2 (see Section 4), showed that while the $\delta^{13}\text{C}$ of the alkyl fragments of the
229 acids reflected the original kerogen, the $\delta^{13}\text{C}$ of the carboxyl carbon was an indication
230 of the isotopic signature of the dissolved inorganic carbon; experimentally proving

231 that the carboxyl carbon in organic acids is readily exchanged with aqueous inorganic
232 carbon.

233 **3.2 Mechanistic study of chemical reactions**

234

235 The occurrence of isotopic fractionation during chemical reactions means that stable
236 isotope can be employed to elucidate mechanistic pathways of reactions [27]. These
237 fractionations are the greatest on the reacting atoms and the KIE on this given position
238 will provide important clues on the nature and therefore the pathway of the reaction.
239 KIEs are not accessible using CSIA and while multiple isotope enrichment factors can
240 sometimes be useful; the method is limited for mechanistic studies.

241 In its simplest form PSIA can be used to investigate the pathway of a single chemical
242 reaction. Oba and Naraoka [28], using a CF-IRMS system similar to System 2 (see
243 Section 4), characterised the ultra violet degradation (UVA and visible) of acetic acid
244 by looking at the changes in $^{13}\text{C}/^{12}\text{C}$ of both the whole molecule and the two carbon
245 positions (the carboxyl carbon and the methyl carbon). PSIA on the acetic acid
246 showed that the isotopic fractionation seen on the whole molecule was mainly
247 attributable to fractionation on the carboxyl carbon, demonstrating that UV exposure
248 might have a notable effect on the carbon stable isotope value of acetic acid present in
249 carbonaceous meteorites. They were also able to determine the position specific
250 enrichment factor values for the carboxyl, which could provide more detailed
251 information on the mechanism.

252 Similarly, Gauchotte *et al.* characterised the permanganate oxidation of methyl *tert*
253 butyl ether (MTBE), a gasoline oxygenate and ubiquitous groundwater contaminant
254 by on-line PSIA, using System 5 (see Section 4)[29]. This enabled to simultaneously
255 obtained $\delta^{13}\text{C}$ values for the two reactive groups in MTBE: the methoxy group and the
256 2-methylpropyl group. Firstly, before reaction the carbon atom of the methoxy group
257 was found to be highly depleted compared to the 2-methylpropyl group, showing that
258 in MTBE the distribution of ^{13}C is non statistical. Secondly, after about several hours
259 of reaction, the $\delta^{13}\text{C}$ of whole molecule MTBE was enriched by 6.2‰, the $\delta^{13}\text{C}$ of the
260 2-methylpropyl group remained unchanged and the $\delta^{13}\text{C}$ of the methoxy group was
261 enriched by 22.8‰ (Figure 2) demonstrating unequivocally that the C-H bonds of the
262 methoxy group are the specific sites of this oxidation [29, 30] This had been the
263 putative reaction pathway but had never been experimentally demonstrated.

264 Non-statistical distribution of ^{13}C in a molecule means that the assumption that the
265 position specific enrichment factor is $\eta\epsilon$ is usually incorrect and that AKIEs calculated
266 using Equation (4) will often be inaccurate. A more appropriate value for the intrinsic
267 enrichment factor should be $(\delta^{13}\text{C}_{\text{total}}/\delta^{13}\text{C}_{\text{position}})\eta\epsilon$, but this is only accessible through
268 PSIA analysis.

269 CSIA has become a very valuable tool over the last couple of decades for the
270 evaluation of the fate of organic contaminants in the subsurface and several excellent
271 reviews have been published in the last ten years [31-33], some focusing particularly
272 on MTBE [18] an exemplar molecule for the technique. Authors have attempted to
273 use CSIA results and particularly whole molecule enrichment factors, determined in
274 laboratory microcosms [32], to calculate AKIEs and estimate new enrichment factors
275 for different contaminants undergoing the same biodegradation process. This was
276 because, as pointed out earlier, theoretically KIEs only depend on the local reaction
277 mechanism and not the nature of the whole molecules. Attempts to experimentally
278 demonstrate the conservation of the AKIEs, however, were not successful [34].
279 Morasch *et al.* presented a study of the anaerobic degradation of m-cresol and p-cresol
280 by *D. cetonicum* on one hand, and of m-xylene and o-xylene by a strain OX39 on the
281 other hand [34]. Both bacterial degradation pathways proceed *via* the formation of
282 benzylsuccinate, with the first step of degradation being a hydrogen substitution on a
283 methyl group of the substrate. All the carbon enrichment factors determined in this
284 study were of the same order of magnitude. When the intrinsic or position specific
285 enrichment factors were calculated, however, they were found different for each
286 contaminant although the first step of reaction was identical. There are several
287 possible reasons that explain these results. The first possible reason is the likely
288 inaccuracy of $\eta\epsilon$ as a value for the intrinsic enrichment factor. But an additional and
289 important possibility is that enzymatic reactions cannot be directly assimilated to
290 chemical reaction in terms of fractionations: there might additional rate-limiting steps
291 such as 1) uptake and migration of compounds in the cell as demonstrated for instance
292 by Nijenhuis *et al* [35]. through the comparison of enrichment factors associated with
293 tetrachloroethylene dechlorination in pure cultures, cell free extracts and pure
294 enzymes, 2) the commitment to catalysis (a measure of the efficiency of the
295 enzymatic reaction) as defined by Northrop [36] and illustrated for example for the
296 biodegradation of chloroethane by Lollar *et al.* [37] or else 3) the substrate-specificity
297 of the reaction with differences in transition states as proposed by Rosell *et al.* in a

298 study of the biodegradation of different gasoline oxygenates [38]. Intrinsic
299 enrichments for enzymatic reactions could be accessible only through PSIA.
300 Additionally, when looking at metabolites that are the products of a multi-enzymes
301 metabolic pathway, the stable isotope signatures reflect multiple sequential isotope
302 effects and their precursors. Bayle *et al.* [39] employed ^{13}C NMR to track and explain
303 the carbon position specific stable isotope distribution in ethanol molecules issued
304 from three different fermentation pathways, showing that the final carbon stable
305 isotope distribution in ethanol was dependent on the catabolism. This study [39] and
306 other similar [12, 40] to this one have shown that position specific isotope
307 distributions in metabolites are pathway-specific and have allowed identifying the
308 rate-limiting steps of the pathways. Currently, ^{13}C isotopic labelling is recognised as
309 the most efficient method for the emerging field of fluxomics: the quantitative study
310 of intracellular fluxes [41]. Coupled with metabolomics, fluxomics attempts to
311 explain cellular phenotype and is expected to have an important impact in particular in
312 biomedical science by facilitating drug discovery [42]. The recent analytical
313 developments in PSIA, however, promise development of fluxomics at natural
314 abundance levels, eliminating the need for complex synthesis of expensive labelled
315 substrates and permitting to investigate all positions simultaneously [42].
316

317 **4 On-line PSIA systems**

318 The two analytical solutions for PSIA are SNIF-NMR, which has been reviewed
319 elsewhere [9, 40, 43], and on-line PSIA using CF-IRMS systems. Although the first
320 on-line PSIA system was reported in 1997 [3], the technology is still in its infancy.
321 There is no commercial system available and a handful of laboratories have modified
322 classic CF systems (Elemental Analysis-IRMS (EA-IRMS) or GC-IRMS) for PSIA
323 studies. They fall into two categories: the systems specific to carboxylic acids and the
324 systems compatible with all volatile and semi-volatile compounds.

325 **4.1 On-line site-specific isotope analysis of carboxylic acids.**

326 Carboxylic acids have been the single most important family of interest in the
327 development of site-specific isotope analysis. Therefore, out of the few reported
328 automated on-line systems for position specific isotope analysis, two are concerned
329 with the decarboxylation of acids and the direct measurement of $\delta^{13}\text{C}_{\text{carboxylic}}$. These

330 systems [26, 44] are based on the high temperature chemolysis of acids, which break
331 down into two pyrolysates: an hydrocarbon and CO₂, *i.e.*, benzoic acid breaks down
332 into benzene and CO₂ [44] and butanoic acid into propane and CO₂ [26].
333 On-line site specific systems developed by Oba and Naraoka [44], System 1 presented
334 in Figure 1, and Dias *et al.* [26] are based on simple modification of classic stable
335 isotope analysis instrumentation. Dias *et al.* modified a GC-c-IRMS by replacing the
336 usual oxidisers in the combustion furnace [26] with small palladium wires as catalysts
337 and adding a small amount of pure hydrogen into the helium stream before the
338 entrance to the furnace. Of the two gases produced by the catalytic pyrolysis, only the
339 CO₂ is carried to the mass spectrometer for $\delta^{13}\text{C}$ measurements. The method was
340 coined gas chromatography-pyrolysis-isotope ratio mass spectrometry (GC-Py-
341 IRMS). In a similar manner, Oba and Naraoka modified an EA-Py-IRMS set-up
342 usually employed for bulk stable isotope analysis (BSIA) [44]. The oxidation reactor
343 of the elemental analyser was replaced with a ceramic tube filled with ceramic
344 granules and the tube was topped with platinum wire, thus replicating a pyrolysis
345 furnace [44]. After the separation of the pyrolysates in a gas chromatography column,
346 only the stable isotopic ratios of the formed CO₂ were measured. Dias *et al.*'s system
347 was designed for low molecular weight organic acids that are compatible with gas
348 chromatography and in the system several acids contained in the same mixture can be
349 analysed in a single run [26] but other types of compounds cannot be analysed. In the
350 most recent version of the instrument [45], System 2 on Figure 1, a switching system
351 was placed at the outlet of the column so that the compounds could be directed either
352 directly into the combustion furnace for compound specific analysis or to the catalytic
353 pyrolysis furnace for PSIA. On the other hand, in System 1 only the site-specific
354 isotopic values of solid acids could be determined and therefore only pure samples
355 and not mixtures can be analysed [44]. While adapted to a certain type of analyses,
356 these systems are not ideally adapted to low concentration complex samples.

357 **4.2 On-line systems with analytical flexibility**

358 Yamada *et al.* developed an on-line system originally for the study of acetic acid. In
359 this system the combustion reactor was not modified [46] instead a deactivated fused-
360 silica capillary housed in a 25cm long heated ceramic tube was placed between the
361 split/splitless injector and the inlet of the capillary column in a GC-c-IRMS apparatus.
362 All compounds entering the injector would simultaneously be pyrolysed and pyrolysis

363 temperatures could be varied. All the pyrolysis fragments or pyrolysates (as opposed
364 to only the carboxylic CO₂ in the previously described systems) were then separated
365 in the column and their stable isotope signatures were obtained by classic combustion-
366 IRMS. This set-up as first described was adapted only to the analysis of pure volatile
367 (low molecular weight) acids because there was no means for on-line purification of a
368 single compounds out of mixtures [46]. The authors developed an improved version,
369 System 3 in Figure 1, in which the pyrolysis furnace was placed after the capillary
370 column in a first GC and the pyrolysates were separated in a capillary column placed
371 in a second GC, before being directed to the combustion furnace [21]. The
372 *intramolecular* carbon stable isotopes ratios in acetic acid and ethanol have been
373 investigated with this system [22, 23]. The main disadvantage of this approach,
374 however, is the impossibility to formally identify pyrolysates.

375 Corso and Brenna, pioneers of on-line PSIA, were the first to present a system with
376 real analytical flexibility [3]. It was not designed for any particular application but to
377 be compatible with a wide range of volatile compounds of interest. This system,
378 System 4 on Figure 1, adapted from gas chromatography-pyrolysis-gas
379 chromatography (GC-Py-GC) as first described by Dhont (1961) [47] constitutes of a
380 first gas chromatograph coupled with an inert pyrolysis reactor, which is in turn
381 coupled with a hybrid GC-c-IRMS/ion trap mass spectrometer system. An automated
382 four-port three-way valve placed at the outlet of the first capillary column enables to
383 direct the flow toward either a flame ionisation detector (FID) or a pyrolysis reactor.
384 The FID is used for quantitative analysis of compounds of interest. A fourth port of
385 the valve attached to a second injector allows for direct pyrolysis of pure samples.
386 Similarly to the system of Yamada *et al.*, the pyrolysis reactor is a piece of
387 deactivated fused silica joining the two gas chromatographs through a high
388 temperature furnace and a heated transfer line on each side. Pyrolysis temperature can
389 be adjusted. Additionally, a four-port three-way valve directs the effluent from the
390 second capillary column to either the mass spectrometer for molecular identification
391 of the pyrolysates or to combustion furnace and the IRMS.

392 The high flexibility of the system stems not only from the fact that the breakdown of
393 the molecules of interest into smaller fragments is based on non-catalytic non-specific
394 pyrolysis but also that all these fragments can be both identified in the ion trap mass
395 spectrometer and analysed through the IRMS for isotopic signatures. This system has
396 been used to date for the study of standards of a variety of compounds: fatty acid

397 methyl esters (through the example of methyl palmitate) [3], fatty alcohol (through the
398 example of 1-hexanodecanol) [48], n-alkanes, toluene [49], the analogues of four
399 amino acids: leucine, methionine [24], alanine and phenylalanine [25] and an
400 analogue of lactic acid [50].

401 Gauchotte *et al.* also presented a flexible on-line PSIA system [29], System 5 on
402 Figure 1. While the set-up is similar to System 4, the design of the pyrolysis reactor is
403 significantly different. It is constructed of a quartz tube embedded in a temperature-
404 controlled furnace. At the inlet of the reactor a tee union joins the end of the first
405 capillary column, the quartz tube and a secondary helium supply while at the outlet an
406 open-split was placed to release some of the pressure due to the added helium flow.
407 While in previous systems, the transit time of the sample in the pyrolysis reactor
408 depended only on its dimensions and could not be varied separately from the flow rate
409 in the first capillary column, in this reactor the transit time can be varied by
410 modification of the flow of added helium; giving greater control on the pyrolysis
411 process. The system is also equipped with a liquid nitrogen cryo-trap placed after the
412 pyrolysis reactor to ensure that all pyrolysates are focused when entering the second
413 GC. The system has been used for the study of intramolecular carbon isotope
414 variations in MTBE [29, 30].

415 **5 Fragmentation processes and isotopic** 416 **representativeness.**

417 The breakdown of molecules of interest for on-line site-specific isotope analysis has
418 been conducted in all reported on-line PSIA systems by high temperature chemolysis.
419 The main issues are therefore to identify what moiety or moieties in the parent
420 molecule the fragments originate from and how their carbon stable isotopic signatures
421 relate. Ideally, the conversion should be total (quantitative), each fragment should
422 represent a “slice” of the parent molecule without rearrangement and should not be
423 involved in secondary reactions as it will affect their isotopic ratios. In this case only,
424 the isotopic signatures of the fragments and corresponding moieties would be strictly
425 equal and isotopic representativeness would be total. In most reported cases, however,
426 these conditions were not fulfilled. First, secondary reactions might start before the
427 primary reaction is total, destructing the isotopic representativeness of the pyrolysates.
428 Secondly, scrambling might occur affecting what Sacks and Brenna coined “the
429 structural fidelity” of the fragments: “the extent to which the isotope ratio of a

430 fragment reflects the isotope ratio of a specific position or moiety in the parent
431 compound”[24]. Minimising these various effects means that at optimal pyrolysis
432 conditions, f is generally below one and this means that isotopic fractionation might
433 exist between parents and fragments.

434 The fragmentation mechanisms for reported online PSIA applications fall under three
435 main categories: simple fragmentation of small molecules, non-ideal fragmentation of
436 small molecules and fragmentation of long chain molecules. Table 2 presents an
437 exhaustive summary of reported on-line fragmentation of molecules for PSIA and in
438 this section, we discuss these mechanisms and the different strategies employed to
439 address the various issues highlighted above. It is expected that fragmentation of new
440 compounds for novel on-line PSIA applications would fall within one of these
441 categories.

442

443

444 **5.1 Simple fragmentation of small molecules**

445

446 Here, we defined “simple fragmentation” of a molecule as the straight-forward
447 cleavage of covalent bonds. Structural fidelity of fragmentation is 100% but isotopic
448 representativeness might be affected when fragments are involved in secondary
449 pyrolysis reactions (further fragmentations or polymerisation) or by isotopic
450 fractionation when, in the ideal fragmentation conditions, the reaction is not
451 quantitative.

452 As discussed in Section 4, on-line thermal decarboxylation of acid lead to the
453 formation of a hydrocarbon and CO_2 . In these cases, only the $\delta^{13}\text{C}_{\text{carboxylic}}$ was
454 experimentally determined while the $\delta^{13}\text{C}$ of the complementary hydrocarbon was
455 deduced from a mass conservation calculation using $\delta^{13}\text{C}_{\text{carboxylic}}$ and the $\delta^{13}\text{C}$ of the
456 whole molecule. The main factor affecting the isotopic representativeness of the
457 reported PSIA values was therefore the yield of the decarboxylation reaction.

458 The decarboxylation reactions employed in both cases were different. Oba and
459 Naraoka’s reaction was based solely on thermal decomposition [44]. For the three
460 studied aromatic carboxylic acids, the reaction appeared to be at first a simple
461 breakdown of the bond between the carboxylic carbon atom and the rest of the
462 molecule thus forming CO_2 (Table 2). At high temperatures however, carbon

463 monoxide (CO) was also formed competing with the formation of CO₂ and therefore
464 changing the $\delta^{13}\text{C}_{\text{carboxylic}}$ value. To determine optimal temperature, the relative
465 amount of CO₂ (*i.e.* the intensity of the signal of the major ion 44) and the $\delta^{13}\text{C}_{\text{carboxylic}}$
466 (VPDB) were monitored at various temperatures. In all cases the maximum yield for
467 the production of CO₂ was reached at around 750°C and at higher temperatures the
468 amount of CO₂ started decreasing. On the other hand, the $\delta^{13}\text{C}_{\text{carboxylic}}$ values
469 presented a sigmoid curve in function of the temperature, the initial increase explained
470 by the kinetic isotope effect of the pyrolysis reaction before it reached completeness
471 and the second trend, starting when the amount of CO₂ started to decrease [44] due to
472 the secondary formation of the isotopically lighter CO. While the optimal temperature
473 for the pyrolysis appeared to be 750°C, there was no evidence that at this temperature
474 the conversion from the parent molecule to the CO₂ was quantitative and therefore
475 that the measured $\delta^{13}\text{C}$ value for the CO₂ was exactly equal to that of the parent
476 carbon atom in the acid. The accuracy of the obtained $\delta^{13}\text{C}_{\text{carboxylic}}$ was tested by three
477 different approaches. First, it was measured for various injected quantities of the
478 parent compounds and did not appear to vary. Then a liquid acid with known
479 $\delta^{13}\text{C}_{\text{carboxylic}}$ was analysed through the system and the measured value statistically
480 matched the accepted known value [44]. Finally, the $\delta^{13}\text{C}_{\text{carboxylic}}$ values of the acids
481 standards were determined by conventional off-line methods and the results were
482 within 1.0‰ of each other. The obtained stable isotopic values measured by the on-
483 line system could be deemed representative of the actual moiety values.

484 The thermal decarboxylation process used within the GC-Py-IRMS [26] followed a
485 different mechanism as it was helped by the addition of dihydrogen and catalysed by
486 palladium [51]. In this case also, the optimal temperature for the pyrolysis was
487 assumed to be the temperature for which the production of CO₂ was maximal
488 (600°C), however, there was no evidence that the reaction was complete or that
489 secondary reactions did not take place. The isotopic representativeness was partially
490 established by comparison of the results for two unlabelled carboxylic acids with the
491 GC-c-IRMS results of isotopic-dilution linear regressions for two acids with, ¹³C
492 enriched carboxylic positions [26].

493 Yamada *et al.* also reported non-catalysed decarboxylation of acetic acid, producing
494 two main fragments: CO₂ and methane [46]. Other pyrolysis products were also
495 identified such as ethane and propane, which were most likely formed from the
496 polymerisation of methane. The carbon stable isotope ratios of all fragments was

497 measured. Comparison of the $\delta^{13}\text{C}$ values for CO_2 and methane with the $\delta^{13}\text{C}$ values
498 of the two parent moieties determined by off-line PSIA demonstrated that for a
499 pyrolysis temperature of 1000°C while the carbon isotopic value of CO_2 was similar
500 to $\delta^{13}\text{C}_{\text{carboxylic}}$, the $\delta^{13}\text{C}$ value of methane was depleted by almost 3‰ compared to
501 $\delta^{13}\text{C}_{\text{methyl}}$. This was possibly because methane was involved in secondary reactions.
502 To overcome the problem associated with the isotopic fractionation due to secondary
503 reaction, the $\delta^{13}\text{C}_{\text{methyl}}$ values were deduced from the subtraction of the $\delta^{13}\text{C}_{\text{carboxylic}}$
504 from the bulk isotopic value of the acetic acid [46].

505 Gilbert *et al.* [23] optimised the pyrolysis of ethanol. It was shown to occur through
506 two reactions: a dehydration producing ethylene and water and the breakdown of the
507 central C-C bond to form methane and CO. Using 14 different ethanol samples for
508 which the *intramolecular* distribution had been determined through an off-line
509 method, it was shown that for the breaking of the C-C bond, the CO fragment was
510 always depleted compared with the original moiety in the ethanol molecule while the
511 methane fragment was always enriched. The enrichment, and hence the fractionation
512 appeared, however, constant in all 14 samples which enabled to establish correction
513 factors and to obtain $\delta^{13}\text{C}_{\text{VPDB}}$ values of the two moieties. The authors also
514 demonstrated that the observed ethylene did not originate solely from the dehydration
515 reaction but also from the polymerisation of methane and therefore should be ignored
516 for PSIA of ethanol.

517 The on-line pyrolysis of toluene in System 4 [49] presented two fragments: benzene
518 and methane. The pyrolysis reaction was a simple cleavage of the C-C bond between
519 the benzene ring and the methyl group of the toluene as demonstrated by a ratio for
520 the peak areas of the major ion 44 of benzene and methane of 6:1 at 800°C . At this
521 temperature, the reaction yield was very low (Table 2). At higher temperature, the
522 (benzene: methane) ratio was lower due to secondary reactions on benzene. The
523 reconstituted $\delta^{13}\text{C}_{\text{VPDB}}$ value for toluene (calculated based on a Figure presented in
524 [49]) appears depleted of almost 3‰ compared to the measured $\delta^{13}\text{C}$ for the parent
525 molecule, demonstrating that isotopic fractionation occurred during the pyrolysis
526 reaction although it was not quantified by the authors.

527 In System 5, the gaseous on-line pyrolysis of MTBE produced isobutylene and
528 methanol via an intramolecular elimination breaking the C-O bond [29]. The pyrolysis
529 reaction was studied at both various temperatures and various pyrolysis reaction
530 times. Up to 675°C , the formation of the pyrolysates was equal to the consumption of

531 the parent molecule, but at higher temperatures and longer reaction times, the
532 isobutylene and methanol concentrations were lower than that of the consumed
533 MTBE, indicating the occurrence of secondary reactions. At the chosen optimal
534 temperature for the pyrolysis reaction, the reaction was not total and therefore isotopic
535 fractionation was expected. To evaluate the extent of the fractionation and correct the
536 $\delta^{13}\text{C}$ values of the pyrolysates accordingly to obtain accurate $\delta^{13}\text{C}_{\text{VPDB}}$ for the two
537 moieties, the carbon enrichment factor associated with the pyrolysis was measured
538 using the Rayleigh equation (Equation 3). This allowed for a better understanding of
539 the fractionation phenomena in the system. Two types of fractionations were
540 identified. Firstly, a carbon isotopic shift of MTBE between the moment it enters the
541 system and the pyrolysis was evidenced by the difference between the origin ordinate
542 of the Rayleigh plot and the carbon isotopic signature of MTBE before pyrolysis. A
543 first, pre-pyrolysis fractionation was measured. Secondly, using the measured
544 enrichment factor for the pyrolysis, the kinetic isotopic fractionation of the
545 pyrolysates was also calculated. Elucidation of the pyrolysis mechanism and of the
546 two fractionations enabled to establish correction factors linking the carbon stable
547 isotopic values of the pyrolysates to that of their parent moieties. The $\delta^{13}\text{C}$ values of
548 the two MTBE functional groups could be reported against the international standard
549 VPDB and isotopic representativeness established despite the occurrence of
550 fractionation [29].

551 **5.2 Non-ideal fragmentation of small molecules**

552 The fragmentation of a small molecule is qualified as non-ideal when a fragment can
553 be formed by two or more different pyrolysis reactions. Their carbon isotopic
554 signature therefore does not represent the isotopic signature of a “slice” of the parent
555 molecule but rather the mixing signatures from various positions and therefore their
556 structural fidelity is smaller than 100%. For optimal PSIA, the level of structural
557 fidelity of each fragment should be known. Brenna’s team developed a method to
558 measure fidelity for non-ideal fragmentation using isotopically labelled standards. In
559 ideal situations a label standard should be used for each carbon position. The on-line
560 pyrolysis of dilution series of these labelled standards is carried out and the fidelity of
561 the various pyrolysates can be determined using the following equation (Equation
562 (5)):

563

$$R_{fragment} = \sum_{i=1}^n R_i \xi_i = R_{lab} \xi_{lab} + \sum_{i=1}^{n-1} R_i \xi_i \quad (5)$$

Where n is the total number of carbon atoms in the parent molecule, $R_{fragment}$ is the isotope ratio of a fragment, R_i , the isotope ratio and ξ_i , the fraction of carbon in the product molecule originating from the position i , and R_{lab} and ξ_{lab} are the equivalent value for the labelled position. The term sum of $R_i \xi_i$ is constant for each sample of a dilution series. The slope of the linear regression of $R_{fragment}$ as a function of R_{lab} is ξ_{lab} , the contribution of the labelled carbon atom to the fragment. For most reported molecules (mainly amino acid derivatives) by Brenna *et al.* [24, 25, 50], the fidelity was not 100% and the fragments were identified as originating from various carbon atoms. When the fidelity of all the fragments has been determined, a system of equations can be established. To calculate the isotopic values of n moieties in a molecule, n equations are required, including the mass balance equation of the overall molecule and $n-1$ equations for $n-1$ fragments including at least $n-1$ out of the n carbon atoms. In certain cases, the fidelity might need to be determined at various pyrolysis temperatures to obtain a sufficient number of equations.

In most cases, the fragments with the highest fidelity are formed at temperatures at which the pyrolysis reaction is only partial and isotopic fractionation is therefore likely to occur. Sacks and Brenna [24] proposed to report the isotopic ratios of the fragments and the parent moieties in the sample (*spl*) relatively to a standard (*std*) of the same molecule to cancel out the effect of the pyrolysis-induced fractionation using $\Delta\delta^{13}C$ (*spl*) values (Equation (6)) [24]:

$$\Delta\delta^{13}C(spl) = \delta^{13}C(std) - \delta^{13}C(spl) \quad (6)$$

Indeed, the kinetic fractionation factor, α , from the pyrolysis reaction (Equation 3) depends on parameter such as the temperature, the length of the furnace, the flow rate but not on the original stable isotope ratios in the molecule and thus will be equal for sample and standard.

Wolyniak *et al.* devised a method to estimate absolute *intramolecular* isotopic values for molecules with complex pyrolysis processes through the example of the on-line PSIA of propylene glycol [50]. The total fractionation, α , was first evaluated by comparing the $\delta^{13}C$ of the parent compound to the average $\delta^{13}C$ of the fragments, weighted by the fractional abundance of each fragment. Fragment specific fractionation factors were then estimated by considering the possible scenarios of

596 fractionation, i.e. whether the fractionation happened on one carbon atom in the
597 fragment or was equally distributed amongst the atoms. The $\delta^{13}\text{C}$ value of each
598 fragment was then corrected for pyrolysis fractionation and a new system of equations
599 was established using the new absolute isotopic ratio for the fragments and the same
600 fidelity values and absolute values were obtained for the each of the three carbon
601 atoms with a standard deviation of <3%.

602

603 **5.3 Pyrolysis of long chain molecules**

604 Brenna *et al.* [1, 48, 49] carried out high precision position-specific isotope analysis on
605 a series of aliphatic chain molecules: methyl palmitate, a fatty acid methyl esters
606 (FAMEs), 1-hexadecanol, a fatty alcohol and a series of the n-alkanes (n-pentane,
607 n-hexane, n-heptane, n-octane and n-decane).

608 The long chain molecules fragmented by pyrolysis into two series of fragments that
609 corresponded to the breaking of a single C-C bond along the chain: a ω -
610 monounsaturated methyl ester series and the complementary olefins for methyl
611 palmitate (Me 16:0) and alcohol series and the complementary olefin series for 1-
612 hexadecanol. Carbon rearrangement during pyrolysis was ruled out by carrying out
613 the on-line pyrolysis of compounds isotopically labelled at various positions [52]. The
614 carbon isotopic signatures of the fragment containing the carboxylic or alcohol
615 position follow the mass balance (Equation (7)):

$$616 \quad F_T = \chi_{C1} F_{C1} + (1 - \chi_{C1}) F_R = \chi_{C1} (F_{C1} - F_R) + F_R \quad (7)$$

617 Where F is the ^{13}C fraction and χ the molecular fraction (T=total, C1= the carboxylic
618 or alcohol position and R= all other remaining positions in the fragment). Thus, when
619 plotting F_T in function of χ_{C1} assuming F_R constant, the y-axis intercept (F_R)
620 corresponds to the mean isotope fraction of the molecule excluding the first position
621 while the ^{13}C fraction of the carboxylic or alcohol position is obtained by slope+ F_R .

622 To validate this model for both the FAME and the fatty alcohol, high precision
623 position-specific isotope analysis was carried out on a mixture of unlabelled
624 compounds and [$1\text{-}^{13}\text{C}$] labelled compounds. The isotopic values for the olefins series
625 were uniform and in the expected natural abundance range while the plots for the
626 methyl ester/alcohol series carbon isotopic signatures as a function of the number of
627 carbon atoms had the appearance of a mixing curve. The influence of the labelled
628 position decreasing by dilution with the increase of the fragment molecular size. In

629 the case of methyl palmitate the value obtained for F_R matched closely the mean ^{13}C
630 atomic fraction of the olefins series (excluding methane and ethylene) while the
631 values obtained for F_{C1} corresponded to the value expected after the dilution of the
632 labelled compound. In the case of the fatty alcohol, the correspondence between the
633 calculated F_R value and the average ^{13}C atomic fraction for the olefins series presented
634 a difference equivalent to around 6%. This provided evidence of fractionation of the
635 parent compound, which the authors attributed to the competing formation of a
636 dehydration product present on the pyrolysates chromatogram.

637 The n-alkanes also broke down in complementary series [49]. Each alkane fragmented
638 into a series of straight-chain hydrocarbons separated by one carbon unit ranging from
639 the methane to the parent compound. The study of the peak area percentage of the
640 alkane fragments presented evidence of secondary pyrolysis reactions that implied
641 that the isotopic representativeness of the measurement was affected. To measure the
642 overall discrepancy between the fragments isotopic signatures and the parent
643 compound, Brenna *et al.* [49] proposed to calculate the mean of the weighed averages
644 of the isotope ratios of complementary fragments (two fragments for which the
645 combination of carbon atom numbers adds up to the number of carbon atoms in the
646 parent molecule) and to compare it to the isotope ratio of the parent compound. For
647 both the alkanes and the 1-hexanodecanol, this method unveiled small but statistically
648 significant differences. These could be due to possible secondary reactions but also to
649 the kinetic isotope effect of the pyrolysis, which in all cases was not quantitative. In
650 fact, comparison of the pyrolysis fragments isotopic signatures at different pyrolysis
651 temperatures [49, 52] divulged slight differences. While optimal pyrolysis
652 temperatures were chosen to minimise the possibility of a secondary reaction, i.e.
653 smaller yields, it meant that the kinetic isotope effect of the pyrolysis was more
654 important but was not quantified.

655 **6 Precision and sensitivity**

656 On-line PSIA systems are part of the interface development that followed the
657 invention of continuous flow IRMS systems. Continuous flow systems are less precise
658 than dual inlet systems but have better sensitivity. In order to be successful continuous
659 flow devices, PSIA systems must offer precision and sensitivity equivalent to other
660 systems.

661 In most cases, when the pyrolysis is not complete, isotopic representativeness of the
662 carbon isotopic values for the moieties (i.e. an accurate VPDB value) can be obtained
663 only if the extent and the location of the isotopic fractionation are known. The
664 reported precision is therefore usually the precision on the measured $\delta^{13}\text{C}$ value for
665 the pyrolysates or for $\Delta\delta^{13}\text{C}$ (*spl*) and not for the $\delta^{13}\text{C}$ of the moiety in the parent
666 compound. For most on-line PSIA systems, the instrumental precision is unchanged
667 compared to a classic GC-c-IRMS (Table 3) and is around $1\sigma = 0.4\text{‰}$. Reported
668 precision for $\Delta\delta^{13}\text{C}$ (*spl*) values in System 4 is similar. When attempting to account
669 for the isotopic fractionation by theoretical calculations, Wolyniak *et al.* then reported
670 a precision of $1\sigma < 3.0\text{‰}$ [25]. When correction factors were calculated between the
671 $\delta^{13}\text{C}$ values of the pyrolysis products and that of the parent moiety using the Rayleigh
672 equation of the pyrolysis, error propagation on the experimentally derived terms
673 meant that the overall precision was a 95% confidence interval of 0.5‰ [29].
674 The sensitivity of PSIA system can be affected by three main factors: the number of
675 carbon atoms in the fragment, the yield of the pyrolysis reaction and the addition of
676 gas through the system. In most devices apart from System 5 the mass of gas through
677 the system is not different to that of a classic GC-c-IRMS. When the pyrolysis
678 reaction is quantitative the sensitivity should only be affected by the fact that the
679 pyrolysates present a smaller amount of carbon atoms than the parent molecule and
680 thus have a smaller IRMS signal [45]. The sensitivity is limited by the number of
681 carbon atoms in the smallest fragment. For instance, if a molecule containing seven
682 carbon atoms breaks down into one fragment containing five carbon atoms and one
683 containing two carbon atoms, the sensitivity of on-line PSIA compared to CSIA of the
684 same molecule will be decreased by 71% (2/7). In many cases, however, the optimal
685 conditions for pyrolysis correspond to condition when the reaction is not total and $f < 1$
686 (Table 2), which means that the sensitivity is further affected by the low production of
687 pyrolysates. For instance, if for the same pyrolysis reaction, the remaining fraction of
688 reactant at optimal temperature is 40% then the sensitivity is further decreased by
689 60% and the total loss of sensitivity is around 85%. Therefore, by the nature of the
690 analysis on-line PSIA detection limits are higher than for classic CSIA systems
691 presenting a clear limitation to the method. Reported precisions and sensitivity for
692 existing systems are presented in Table 3.
693

694 **7 Conclusions**

695 PSIA has been identified by leading isotope researchers along with clumped isotopes
696 as the future for isotopic research [53]. The applications of the technique span across a
697 very wide range of topics. While in astrobiology it could help elucidate the origin of
698 life on Earth in biochemistry it could become an invaluable tool to complement the
699 emerging ‘omics approaches.

700 And while its potential was first unveiled several decades ago [7], the analytical
701 difficulties intrinsic to the measurements notably in complex mixtures and at trace
702 level have for a long time limited its development. PSIA techniques using CF-IRMS
703 and SNIF NMR are now employed by a handful of laboratories and applications are
704 multiplying. Tellingly, Yamada *et al.* [54] have now developed reference materials for
705 acetic acid on-line PSIA studies in order to facilitate inter-laboratory and inter-method
706 calibration; demonstrating a more routine future for the technique.

707

708

709 **List of Figures:**

710

711 **Figure 1- On-line PSIA systems developed from CF-IRMS instrumentation.**

712 Systems 1 and 2 permit on-line decarboxylation of acids and provide direct
713 measurements of the carbon stable isotope ratios of the carboxylic carbon atom.
714 Systems 3, 4 and 5 are non-specific systems and have been employed for a wide range
715 of organic compounds. The three systems are constituted of two GCs enabling the
716 isolation of the compound of interest in the first GC and the separation and CSIA of
717 its fragmentation compounds through the second GC. **a:** Pyrolysis chamber consisting
718 of a ceramic tube containing deactivated fused silica, **b:** Pyrolysis chamber consisting
719 of a ceramic tube containing ceramic granules with 30cm of platinum wire crumpled
720 on top of the granules, **c:** Pyrolysis chamber consisting of a quartz tube with capillary
721 column inserted into both ends of the tube, **d:** Pyrolysis chamber consisting of
722 ceramic alumina tube filled with four palladium wires, **e:** Combustion furnace, **f:** 4
723 port Valco valve, **g:** GC column, **h:** Back flush system

724

725

726 **Figure 2- Changes (Δ) in carbon stable isotope ratios of MTBE and its**

727 **pyrolysates (methanol and isobutylene) in System 4 during permanganate**
728 **oxidation of MTBE (Reproduced from [30]).** The signature of the pyrolysate
729 (isobutylene) representative of the non-reacting position remained unchanged while
730 that of the pyrolysate representative of the carbon atom at the first site of attack
731 (methanol) became greatly enriched.

732

733 **List of Tables:**

734

735 **Table 1- Levels of specificity in stable isotope analysis.**

736

737 **Table 2- Fragmentation of organic compounds in on-line PSIA systems.** The

738 compounds are categorized by fragmentation mechanisms. ¹f is the remaining fraction
739 of reactant at optimal fragmentation conditions. ² 100% structural fidelity means that
740 the isotope ratio of a fragment uniquely originates from the isotope ratio of a specific
741 position in the parent compound. ³ System numbers refer to numbers presented in
742 Figure 1. n.r.= non reported

743

744 **Table 3- Reported precisions and sensitivity of the on-line PSIA systems.** ¹

745 System numbers refer to numbers presented in Figure 1.

746

747

748

749

750

751 **Acknowledgments**

752 The authors would like to thank the EPSRC for financial support through grants
753 EP/D013739/1 and EP/D013739/2, the Royal Society for the Paul Instrument Fund
754 Fellowship granted to CGL and the University of Glasgow for SMT's PhD
755 studentship.

756

757

758

759

760 **Uncategorized References**

761 [1] J.T. Brenna, T.N. Corso, H.J. Tobias, R.J. Caimi, High-precision continuous-flow
762 isotope ratio mass spectrometry, *Mass Spectrom Rev*, 16 (1997) 227-258.

763 [2] W. Meier-Augenstein, Applied gas chromatography coupled to isotope ratio mass
764 spectrometry, *Journal of chromatography. A*, 842 (1999) 351-371.

765 [3] T.N. Corso, J.T. Brenna, High-precision position-specific isotope analysis,
766 *Proceedings of the National Academy of Sciences*, 94 (1997) 1049-1053.

767 [4] S. Benson, C. Lennard, P. Maynard, C. Roux, Forensic applications of isotope
768 ratio mass spectrometry—a review, *Forensic science international*, 157 (2006) 1-22.

769 [5] L.C. Melander, W.H. Saunders, *Reaction rates of isotopic molecules*, Wiley New
770 York 1980.

771 [6] K.D. Monson, J.M. Hayes, Carbon isotopic fractionation in the biosynthesis of
772 bacterial fatty acids. Ozonolysis of unsaturated fatty acids as a means of determining
773 the intramolecular distribution of carbon isotopes, *Geochimica et Cosmochimica*
774 *Acta*, 46 (1982) 139-149.

775 [7] P.H. Abelson, T.C. Hoering, Carbon Isotope Fractionation in Formation of Amino
776 Acids by Photosynthetic Organisms, *P Natl Acad Sci USA*, 47 (1961) 623-&.

777 [8] T. Weilacher, G. Gleixner, H.-L. Schmidt, Carbon isotope pattern in purine
778 alkaloids a key to isotope discriminations in C1 compounds, *Phytochemistry*, 41
779 (1996) 1073-1077.

780 [9] G.J. Martin, S. Akoka, M.L. Martin, SNIF-NMR—Part 1: Principles, *Modern*
781 *Magnetic Resonance*, Springer 2006, pp. 1651-1658.

782 [10] M.L. Martin, G.J. Martin, Site-specific isotope effects and origin inference,
783 *Analisis*, 27 (1999) 209-213.

784 [11] V. Caer, M. Trierweiler, G.J. Martin, M.L. Martin, Determination of site-specific
785 carbon isotope ratios at natural abundance by carbon-13 nuclear magnetic resonance
786 spectroscopy, *Analytical chemistry*, 63 (1991) 2306-2313.

787 [12] A. Gilbert, R. Hattori, V. Silvestre, N. Wasano, S. Akoka, S. Hirano, K. Yamada,
788 N. Yoshida, G.S. Remaud, Comparison of IRMS and NMR spectrometry for the
789 determination of intramolecular ^{13}C isotope composition: Application to ethanol,
790 *Talanta*, 99 (2012) 1035-1039.

791 [13] S. Asche, A.L. Michaud, J.T. Brenna, Sourcing organic compounds based on
792 natural isotopic variations measured by high precision isotope ratio mass
793 spectrometry, *Current Organic Chemistry*, 7 (2003) 1527-1543.

794 [14] J.T. Brenna, Natural intramolecular isotope measurements in physiology:
795 elements of the case for an effort toward high-precision position-specific isotope
796 analysis, *Rapid Communications in Mass Spectrometry*, 15 (2001) 1252-1262.

797 [15] M. Elsner, L. Zwank, D. Hunkeler, R.P. Schwarzenbach, A new concept linking
798 observable stable isotope fractionation to transformation pathways of organic
799 pollutants, *Environmental science & technology*, 39 (2005) 6896-6916.

800 [16] A.S. Burton, J.C. Stern, J.E. Elsila, D.P. Glavin, J.P. Dworkin, Understanding
801 prebiotic chemistry through the analysis of extraterrestrial amino acids and
802 nucleobases in meteorites, *Chemical Society Reviews*, 41 (2012) 5459-5472.

803 [17] A. Mariotti, J. Germon, P. Hubert, P. Kaiser, R. Letolle, A. Tardieux, P.
804 Tardieux, Experimental determination of nitrogen kinetic isotope fractionation: some
805 principles; illustration for the denitrification and nitrification processes, *Plant and soil*,
806 62 (1981) 413-430.

807 [18] L. Zwank, M. Berg, M. Elsner, T.C. Schmidt, R.P. Schwarzenbach, S.B.
808 Haderlein, New Evaluation Scheme for Two-Dimensional Isotope Analysis to
809 Decipher Biodegradation Processes: Application to Groundwater Contamination by
810 MTBE, *Environmental Science & Technology*, 39 (2005) 1018-1029.

811 [19] L.M. Reid, C.P. O'Donnell, G. Downey, Recent technological advances for the
812 determination of food authenticity, *Trends in Food Science & Technology*, 17 (2006)
813 344-353.

814 [20] S. Armellin, E. Brenna, S. Frigoli, G. Fronza, C. Fuganti, D. Mussida,
815 Determination of the synthetic origin of methamphetamine samples by ^2H NMR
816 spectroscopy, *Analytical chemistry*, 78 (2006) 3113-3117.

817 [21] U. Bussy, C. Thibaudeau, F. Thomas, J.-R. Desmurs, E. Jamin, G.S. Remaud, V.
818 Silvestre, S. Akoka, Isotopic finger-printing of active pharmaceutical ingredients by
819 ^{13}C NMR and polarization transfer techniques as a tool to fight against
820 counterfeiting, *Talanta*, 85 (2011) 1909-1914.

821 [22] R. Hattori, K. Yamada, M. Kikuchi, S. Hirano, N. Yoshida, Intramolecular
822 carbon isotope distribution of acetic acid in vinegar, *Journal of agricultural and food*
823 *chemistry*, 59 (2011) 9049-9053.

824 [23] A. Gilbert, K. Yamada, N. Yoshida, Accurate method for the determination of
825 intramolecular ^{13}C isotope composition of ethanol from aqueous solutions, *Anal*
826 *Chem*, 85 (2013) 6566-6570.

827 [24] G.L. Sacks, J.T. Brenna, High-Precision Position-Specific Isotope Analysis
828 of $^{13}\text{C}/^{12}\text{C}$ in Leucine and Methionine Analogues, *Analytical Chemistry*, 75 (2003)
829 5495-5503.

830 [25] C.J. Wolyniak, G.L. Sacks, B.S. Pan, J.T. Brenna, Carbon position-specific
831 isotope analysis of alanine and phenylalanine analogues exhibiting nonideal pyrolytic
832 fragmentation, *Anal Chem*, 77 (2005) 1746-1752.

833 [26] R.F. Dias, K.H. Freeman, S.G. Franks, Gas chromatography-pyrolysis-isotope
834 ratio mass spectrometry: a new method for investigating intramolecular isotopic
835 variation in low molecular weight organic acids, *Organic Geochemistry*, 33 (2002)
836 161-168.

837 [27] B.-L. Zhang, S. Buddrus, M.L. Martin, Site-specific hydrogen isotope
838 fractionation in the biosynthesis of glycerol, *Bioorganic Chemistry*, 28 (2000) 1-15.
839 [28] Y. Oba, H. Naraoka, Carbon and hydrogen isotope fractionation of acetic acid
840 during degradation by ultraviolet light, *Geochemical Journal*, 41 (2007) 103-110.
841 [29] C. Gauchotte, G. O'Sullivan, S. Davis, R.M. Kalin, Development of an advanced
842 on-line position-specific stable carbon isotope system and application to methyl tert-
843 butyl ether, *Rapid Communications in Mass Spectrometry*, 23 (2009) 3183-3193.
844 [30] C. Gauchotte, G. Connal, G. O'Sullivan, R.M. Kalin, Position Specific Isotope
845 Analysis: The Ultimate Tool in Environmental Forensics?, *Environmental Forensics :
846 Proceedings of the 2009 INEF Annual Conference*, RSC Publishing 2010, pp. 60-70.
847 [31] T.B. Hofstetter, M. Berg, Assessing transformation processes of organic
848 contaminants by compound-specific stable isotope analysis, *Trac-Trend Anal Chem*,
849 30 (2011) 618-627.
850 [32] R.U. Meckenstock, B. Morasch, C. Griebler, H.H. Richnow, Stable isotope
851 fractionation analysis as a tool to monitor biodegradation in contaminated aquifers,
852 *Journal of Contaminant Hydrology*, 75 (2004) 215-255.
853 [33] T.C. Schmidt, H.-A. Duong, M. Berg, S.B. Haderlein, Analysis of fuel
854 oxygenates in the environment, *Analyst*, 126 (2001) 405-413.
855 [34] B. Morasch, H.H. Richnow, A. Vieth, B. Schink, R.U. Meckenstock, Stable
856 isotope fractionation caused by glycol radical enzymes during bacterial degradation of
857 aromatic compounds, *Appl Environ Microbiol*, 70 (2004) 2935-2940.
858 [35] I. Nijenhuis, J. Andert, K. Beck, M. Kästner, G. Diekert, H.-H. Richnow, Stable
859 isotope fractionation of tetrachloroethene during reductive dechlorination by
860 *Sulfurospirillum multivorans* and *Desulfitobacterium* sp. strain PCE-S and abiotic
861 reactions with cyanocobalamin, *Applied and Environmental Microbiology*, 71 (2005)
862 3413-3419.
863 [36] D.B. Northrop, The expression of isotope effects on enzyme-catalyzed reactions,
864 *Annual review of biochemistry*, 50 (1981) 103-131.
865 [37] B.S. Lollar, S. Hirschorn, S.O. Mundle, A. Grostern, E.A. Edwards, G.
866 Lacrampe-Couloume, Insights into enzyme kinetics of chloroethane biodegradation
867 using compound specific stable isotopes, *Environmental science & technology*, 44
868 (2010) 7498-7503.
869 [38] M. Rosell, R. Gonzalez-Olmos, T. Rohwerder, K. Rusevova, A. Georgi, F.D.
870 Kopinke, H.H. Richnow, Critical evaluation of the 2D-CSIA scheme for
871 distinguishing fuel oxygenate degradation reaction mechanisms, *Environ Sci Technol*,
872 46 (2012) 4757-4766.
873 [39] K. Bayle, S. Akoka, G.S. Remaud, R.J. Robins, Non-Statistical ¹³C Distribution
874 during Carbon Transfer from Glucose to Ethanol During Fermentation is Determined
875 by the Catabolic Pathway Exploited, *Journal of Biological Chemistry*, DOI (2014)
876 jbc. M114. 621441.
877 [40] M. Martin, B. Zhang, G.J. Martin, SNIF-NMR—Part 2: Isotope Ratios as Tracers
878 of Chemical and Biochemical Mechanistic Pathways, *Modern Magnetic Resonance*,
879 Springer 2006, pp. 1659-1667.
880 [41] S. Klein, E. Heinzle, Isotope labeling experiments in metabolomics and
881 fluxomics, *Wiley Interdisciplinary Reviews: Systems Biology and Medicine*, 4 (2012)
882 261-272.
883 [42] M. Cascante, S. Marin, Metabolomics and fluxomics approaches, *Essays
884 Biochem*, 45 (2008) 67-82.

885 [43] G.J. Martin, M.L. Martin, G. Remaud, SNIF-NMR—Part 3: From Mechanistic
886 Affiliation to Origin Inference, *Modern Magnetic Resonance*, Springer2006, pp.
887 1669-1680.

888 [44] Y. Oba, H. Naraoka, Site-specific carbon isotope analysis of aromatic carboxylic
889 acids by elemental analysis/pyrolysis/isotope ratio mass spectrometry, *Rapid*
890 *Communications in Mass Spectrometry*, 20 (2006) 3649-3653.

891 [45] B. Thomas, K.H. Freeman, M.A. Arthur, Intramolecular carbon isotopic analysis
892 of acetic acid by direct injection of aqueous solution, *Organic Geochemistry*, 40
893 (2009) 195-200.

894 [46] K. Yamada, M. Tanaka, F. Nakagawa, N. Yoshida, On-line measurement of
895 intramolecular carbon isotope distribution of acetic acid by continuous-flow isotope
896 ratio mass spectrometry, *Rapid communications in mass spectrometry : RCM*, 16
897 (2002) 1059-1064.

898 [47] J. Dhont, *Chromatographic behavior of 2, 4-dinitrophenylhydrazones on*
899 *chromatoplates*, Royal Soc Chemistry Thomas Graham House, Science park, Milton
900 Rd, Cambridge CB4 0WF, Cambs, England, 1961, pp. 74-&.

901 [48] T.N. Corso, B.A. Lewis, J.T. Brenna, Reduction of Fatty Acid Methyl Esters to
902 Fatty Alcohols To Improve Volatility for Isotopic Analysis without Extraneous
903 Carbon, *Analytical Chemistry*, 70 (1998) 3752-3756.

904 [49] T.N. Corso, J.T. Brenna, On-line pyrolysis of hydrocarbons coupled to high-
905 precision carbon isotope ratio analysis, *Analytica Chimica Acta*, 397 (1999) 217-224.

906 [50] C.J. Wolyniak, G.L. Sacks, S.K. Metzger, J.T. Brenna, Determination of
907 Intramolecular $\delta^{13}\text{C}$ from incomplete pyrolysis fragments. Evaluation of
908 pyrolysis-induced isotopic fractionation in fragments from the lactic acid analogue
909 propylene glycol, *Anal Chem*, 78 (2006) 2752-2757.

910 [51] W.F. Maier, W. Roth, I. Thies, P.V.R. Schleyer, Hydrogenolysis, IV. Gas phase
911 decarboxylation of carboxylic acids, *Chemische Berichte*, 115 (1982) 808-812.


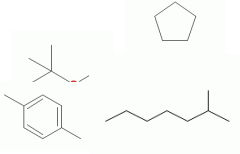
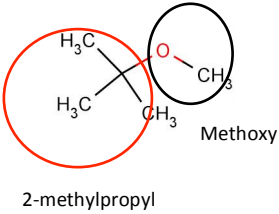
912 [52] T.N.C. J.T.Brenna, H.J.Tobias, R.J.Calmi, High-precision continuous-flow
913 isotope ratio mass spectrometry, *Mass Spectrometry Reviews*, 16 (1997) 227-258.

914 [53] J.M. Eiler, *The Isotopic Anatomies of Molecules and Minerals*, *Annu Rev Earth*
915 *Pl Sc*, 41 (2013) 411-441.

916 [54] K. Yamada, M. Kikuchi, A. Gilbert, N. Yoshida, N. Wasano, R. Hattori, S.
917 Hirano, Evaluation of commercially available reagents as a reference material for
918 intramolecular carbon isotopic measurements of acetic acid, *Rapid Communications*
919 *in Mass Spectrometry*, 28 (2014) 1821-1828.

920

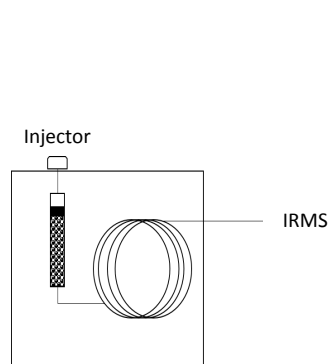
Table 1-

Stable Isotope Analysis	Details	Example	Techniques
Bulk Isotope Analysis (BSIA)	Weighted average isotopic signature of the components of the sample	$\delta^{13}\text{C}$ of gasoline samples 	<ul style="list-style-type: none"> Off-line transformation of the sample gases and analysis in dual inlet IRMS Continuous flow EA-IRMS/TC EA-IRMS
Compound Specific Isotope Analysis (CSIA)	Isotopic signatures of the individual compounds of a mixture- <i>Intermolecular</i> isotopic variations	$\delta^{13}\text{C}$ of individual compounds of gasoline such as methyl <i>tert</i> butyl ether, ethyl <i>tert</i> butyl ether, benzene, toluene, xylenes 	<ul style="list-style-type: none"> Off-line extraction of a mixture and analysis by EA-IRMS TC/EA-IRMS Continuous Flow GC-IRMS
Position Specific Isotope Analysis (PSIA)	Isotopic signatures of different moieties in a molecule- <i>Intramolecular</i> isotopic variations	$\delta^{13}\text{C}$ of the two methyl <i>tert</i> butyl ether moieties 	<ul style="list-style-type: none"> Off-line transformation of a functional group into a simple gas (CO_2) and analysis by dual inlet IRMS Off-line breakdown (chemolysis, pyrolysis) of a molecule and analysis by GC-IRMS of the fragments SNIF-NMR On-line PSIA using CF-IRMS

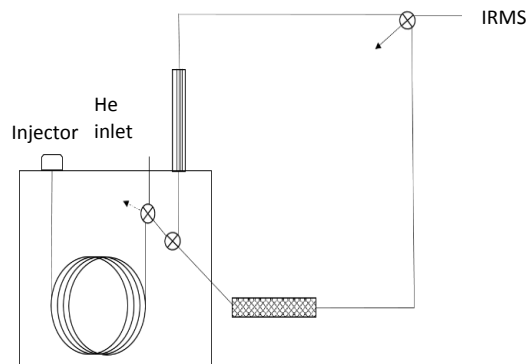
Type of Compounds	Compound	Fragmentation Products	Fragmentation Mechanisms	Optimum Fragmentation Temperature	f ¹	Secondary Reactions	100% Fidelity ²	System ³	Ref
<i>Simple fragmentation of small molecules</i>	Benzoic acid	Benzene and carbon dioxide	Decarboxylation	750°C	n.r.	No	Yes	1	[44]
	Naphthylactic acid	Naphthalene and carbon dioxide	Decarboxylation	750°C	n.r.	No	Yes	1	[44]
	1-Pyrenecarboxylic acid	Pyrene and carbon dioxide	Decarboxylation	750°C	n.r.	No	Yes	1	[44]
	Acetic acid	Methane and carbon dioxide	Decarboxylation	600°C	n.r.	No	Yes	2	[45]
	Acetic acid	Methane and carbon dioxide	Pd-catalysed Decarboxylation with hydrogen	960°C	n.r.	No	Yes	3	[22]
	Methyl <i>tert</i> butyl ether	Methanol and isobutylene	Pyrolysis: Cleavage of the C-O bond by intramolecular elimination	675°C	7-40%	Yes	Yes	5	[29]
	Ethanol	Carbon monoxide, methane, water and ethylene	Pyrolysis 1) Dehydration 2) Cleavage of the C-C bond.	1000°C	<5%	Yes	Yes	3	[23]
	Toluene	Benzene and methane	Pyrolysis Cleavage of the C-C bond between the benzene ring and the methyl group of toluene	800°C	97%	Yes	Yes	4	[49]
<i>Non-ideal fragmentation of small molecules</i>	Analogue of Phenylalanine: phenethylamine	Benzene and toluene	Pyrolysis Cleavage of the C-C bond at the benzene ring Scrambling	900°C	n.r.	No	No	4	[25]
	Analogue of Alanine: Alaninol	Carbon monoxide, methane, ethylene, ethane, propylene and acetonitrile	Pyrolysis Cleavage on the methane, amine and alcohol fragments Scrambling	900°C	n.r.	No	No	4	[25]
	Decarboxylated analogue of Methionine: Isoamylamine	Propylene, isobutylene, hydrogen cyanide, acetonitrile	Pyrolysis Cleavage on the methane and amine fragments Scrambling	780°C	6%	Yes	No	4	[24]
	Decrboxylated analogue of Leucine: 3-methylthiopropylamine	Methane, ethane, hydrogen cyanide, acetonitrile	Pyrolysis Cleavage on the methane, amine and sulphide fragments Scrambling	880°C	n.r.	Yes	No	4	[24]
	Lactic acid analogue: Propylene glycol	Methanol, methane, ethylene, acetaldehyde, propylene, ethanol, propanol	Pyrolysis Cleavage on the methane and alcohol fragments Scrambling	700°C	66%	No	No	4	[50]
<i>Pyrolysis of long chain molecules</i>	n-alkanes	α olefin series and ω - unsaturated alcohol series	Pyrolysis Cleavage of a single C-C bond and the formation of complementary fragments	550°C	n.r.	No	Yes	4	[49]
	Hexadecanol	α olefin series and ω - unsaturated alcohol series	Pyrolysis Cleavage of a single C-C bond and the formation of complementary fragments	600°C	n.r.	No	Yes	4	[48]
	FAMES: Methylpalmitate	methyl ester mono unsaturated and α olefin series	Pyrolysis Cleavage of a single C-C bond and the formation of complementary fragments	550°C	80%	No	Yes	4	[3]

System ¹	Reported Precision	Reported Sensitivity	Ref
1	1σ= 0.4‰. Instrumentation precision for the carboxylic carbon	Analysis was carried out with <3μmol of sample on column ≈200 nmol C	[44]
2	1σ=0.7‰ Instrumentation precision for the carboxylic carbon	Not reported	[45]
3	1σ=0.4‰ Instrumentation precision	Analysis was carried out with 11.5 nmol of acetic acid on the column - 23 nmol C	[22]
4	2σ≈0.4‰ for Δδ ¹³ C (<i>spI</i>) of pyrolysates 1σ <3.0‰ for Δδ ¹³ C of moieties.	Analysis carried out with 2 to 4 μg of sample on the column. Sensitivity was limited by the yield of the pyrolysis.	[3] [25]
5	95% confidence = 0.5‰ for δ ¹³ C _{VPDB} values of the two MTBE moieties.	Sensitivity diminished by the addition of helium in the system and the presence of the open-split and limited by the yield of the pyrolysis.	[29]

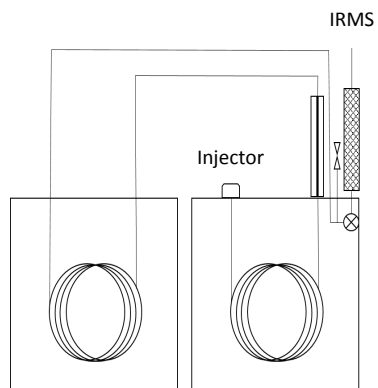
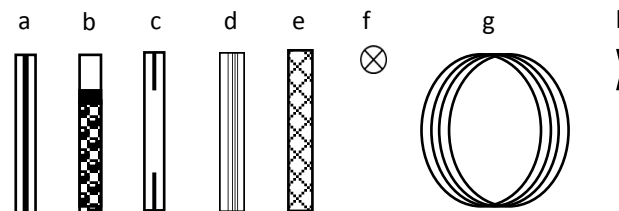
Figure 1



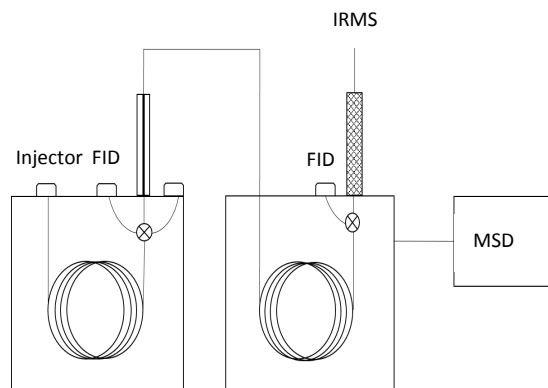
System 1 [44]



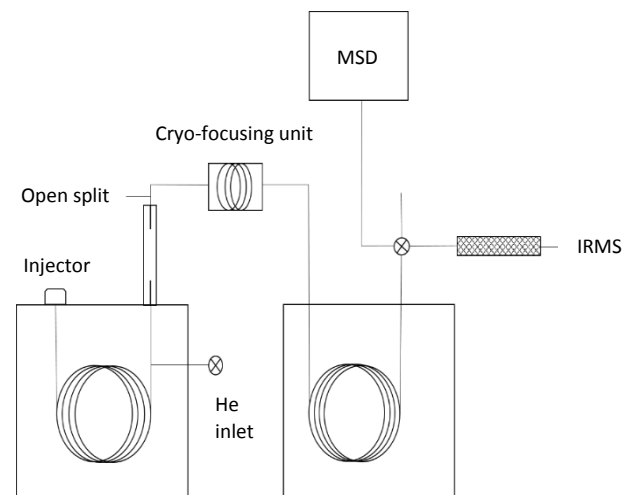
System 2 [45]



System 3 [22]



System 4 [3]



System 5 [29]

Figure 2

